Available online at www.sciencedirect.com

ScienceDirect

journal homepage: www.elsevier.com/locate/he

Hydrogen production from ethylene glycol reforming catalyzed by Ni and Ni–Pt hydrotalcite-derived catalysts

Deborah V. Cesar [a], *Gerardo F. Santori* [b], *Francisco Pompeo* [b], *Maria A. Baldanza* [c], *Cristiane A. Henriques* [a,c], *Eduardo Lombardo* [d], *Martin Schmal* [c], *Laura Cornaglia* [d], *Nora N. Nichio* [b,*]

[a] *UERJ, Instituto de Química, Programa de Pós-graduação em Engenharia Química, Rua São Francisco Xavier, 524 Maracanã, 20550-900 Rio de Janeiro, RJ, Brazil*

[b] *CINDECA, y Facultad de Ingeniería, UNLP-CONICET, 47 N° 257, 1900 La Plata, Argentina*

[c] *NUCAT/PEQ/COPPE-Universidad Federal de Río de Janeiro-Brasil, Cidade Universitaria Centro de Tecnologia, Bloco G, Sala 128, Caixa Postal 68502, 21945-970 Rio de Janeiro, RJ, Brazil*

[d] *INCAPE (FIQ, UNL-CONICET), Santiago del Estero 2829, 3000 Santa Fe, Argentina*

ARTICLE INFO

Article history:
Received 15 June 2016
Received in revised form
18 July 2016
Accepted 19 July 2016
Available online 10 August 2016

Keywords:
Hydrogen
Ethylene glycol
Reforming
Hydrotalcites

ABSTRACT

In this work, we report a study of the steam reforming (SR) and the aqueous phase reforming (APR) of ethylene glycol (EG) with catalysts based on Ni, prepared from hydrotalcite-like compounds. The Pt–Ni bimetallic catalyst was synthesized using controlled techniques derived from Surface Organometallic Chemistry on Metals (SOMC/M). This methodology allows obtaining very well-defined active phases, with low atomic Pt/Ni bulk values (~0.004) and a specific interaction between both metals.

We demonstrate that in the APR of EG, in which the C–O bond cleavage reactions are more favored than in SR, the Ni catalyst is more efficient than the bimetallic Pt–Ni. However, this Pt–Ni bimetallic catalyst is more active and selective to hydrogen in the SR at 450 °C.

The interaction of ethylene glycol with the catalyst surface was studied combining diffuse reflectance infrared spectroscopy with mass spectrometry. Through these studies carried out on the Pt–Ni catalyst, we observed low stability of the formate and carboxylate intermediate species, which would explain its higher activity to produce H_2 and CO_2 through the water gas shift reaction.

Introduction

Nowadays, the search for clean and renewable sources of energy involves an effort to obtain processes using hydrogen such as the reforming of oxygenate molecules. Such compounds, mainly found in the waste streams of bio-based processes (sugars and cellulose) and the aqueous fraction of biomass pyrolysis oil, for instance, are diluted with plenty of water. Therefore, the steam reforming process (SR) requires

* *Corresponding author.*
E-mail address: nnichio@quimica.unlp.edu.ar (N.N. Nichio).
http://dx.doi.org/10.1016/j.ijhydene.2016.07.168

the evaporation of large amounts of water and a reaction temperature higher than 400 °C, which makes it a technology of high energy demand [1,2]. On the other hand, the process of "aqueous phase reforming" (APR) has the advantage of not requiring water evaporation, employing low temperatures (200–250 °C) but high pressures of 20–60 bar. However, the reaction rate is very slow at the low temperatures required for obtaining high hydrogen yields [3]. The catalytic reforming of oxygenated model molecules as ethanol, ethylene glycol and glycerol has also been widely studied [3–12]. In particular, ethylene glycol (EG) is the simplest polyol renewable molecule, and because of its non-volatile nature, it is considered a promising raw material for hydrogen production through reforming reactions [3,8–12]. Furthermore, ethylene glycol (EG) contains the same functional groups present in longer chain polyols, including C–C, C–O, C–H bonds and OH groups on adjacent carbon atoms. The main reactions occurring in the ethylene glycol reforming process are decomposition (1), water gas shift (2) and methanation (3).

$$C_2H_6O_2 \rightarrow 2CO + 3H_2 \quad (1)$$

$$CO + H_2O \rightarrow CO_2 + H_2 \quad (2)$$

$$CO + 3H_2 \rightarrow CH_4 + H_2O \quad (3)$$

The reforming reaction involves the C–C and C–H bonds cleavage to form CO (reaction (1)), which is later converted to CO_2, and in this way, additional H_2 is obtained through the water gas shift (WGS) reaction. Thus, a good catalyst for the reforming process has to be active for the C–C bonds cleavage and for the reaction of WGS and it should not allow the C–O bond cleavage. Through the direct hydrogenation of the CO_x species, CH_4 or superior alkanes could be produced through the Fischer–Tropsch reaction. These parallel reactions produce a decrease in the performance to hydrogen [4].

From a thermodynamic point of view, steam reforming at low temperature (<500 °C) and low steam/oxygenate ratio become adverse for H_2 production and catalyst stability. Under these conditions, the blockage of the active sites through deposition of carbon species could be produced. It has been suggested that the unsaturated C_xH_y species formed through dehydrogenation reactions are coke precursors [6,7]. The CO produced can also form carbon through the Boudouard reaction ($2CO \rightarrow CO_2 + C$). In the APR process, the stability of the catalysts is also affected by leaching and/or sintering of the active phase.

Several studies have been reported on the production of H_2 through ethylene glycol reforming employing Ni catalysts, noble metals like Pt, Rh, Pd and also with bimetallic PtNi, PtCo, and PdFe catalysts [8–12]. According to Cortright et al. [13], high H_2 selectivity can be achieved with Pt/Al_2O_3 catalysts. Vlieger et al. [14] showed that the $Pt–Ni/Al_2O_3$ catalyst improves the H_2 yield because it reduces the formation of alkanes and this improves the catalytic stability.

Huber et al. [15] and Shabaker et al. [16–18] showed that the addition of Sn to Nickel Raney is necessary to avoid alkane formation by methanation. The authors suggest that Sn may block the active sites for CO adsorption and/or dissociation, thus suppressing the undesired methanation reaction. On the other hand, the WGS reaction is promoted, most likely due to the activation of H_2O by Sn. Competition between the methanation and the WGS reactions determines the H_2 selectivity [15–18].

In the case of APR, Vlieger et al. [19] carried out the reaction at 450 °C and 250 bar, with Pt and Pt–Ni catalysts supported on alumina. Methanol, ethanol and acetic acid were the main liquid by-products. They showed that the Pt–Ni bimetallic catalyst reduced the formation of acetic acid and that it has a positive effect on stability. Acetic acid would be responsible for the hydroxylation of the Al_2O_3 support, and the $Al(OH)_x$ species can migrate and cover the metallic particles. Other authors have investigated the formation of glycolic acid and acetic acid employing Pt/ZnO [8] and Co/ZnO catalysts [20].

The use of Ni based or noble metal mixed oxides derived from HTLCs as active catalysts for H_2 production has been extensively studied for the partial oxidation of methane, steam reforming, dry reforming and autothermal reforming of methane at reaction temperatures higher than 650 °C [21,22].

Li et al., studied Ni–Cu/Mg/Al bimetallic catalysts prepared by the calcination and reduction of hydrotalcite-like compounds and were applied for the steam reforming of tar derived from the pyrolysis of biomass at low temperature. They found that the bimetallic catalyst exhibited much higher catalytic activity, better long-term stability and coke resistance than the corresponding monometallic Ni/Mg/Al and Cu/Mg/Al catalysts. The high performance of the bimetallic catalyst was related to its higher metal dispersion, larger amount of surface active sites, higher oxygen affinity, and surface modification caused by the formation of small Ni–Cu alloy particles [23].

Mei et al. studied the steam reforming of ethylene glycol over $MgAl_2O_4$ supported Rh, Ni, and Co catalysts at 500 °C. $MgAl_2O_4$ was chosen as support for its better resistance to carbon formation in steam reforming reactions as compared to Al_2O_3. They found that the CH_4 selectivity on the Co catalyst is much lower than its equilibrium value obtained on the Rh and Ni catalysts. Hence, the $MgAl_2O_4$-supported Co catalyst had a much higher H_2 yield, making it a promising catalyst for EG steam reforming for hydrogen production [24].

The present work reports studies about the steam reforming and the aqueous phase reforming of ethylene glycol with catalysts based on Ni, prepared from hydrotalcite-like compounds (NiHT). Our group has reported that these materials have catalytic properties attractive for the reforming of methane due to their small crystallite size, high surface area, basic properties and good metal dispersion [25]. Since Pt has an excellent activity to the C–C bonds cleavage, the effect of the Pt addition is studied through techniques derived from Surface Organometallic Chemistry on Metals.

The products formed depending on the reaction conditions were also analyzed, which proves essential for the good design of a catalyst. To better understand the catalyst performance, the catalytic activity results were correlated with in situ surface characterization by diffuse reflectance infrared spectroscopy combined with mass spectrometry (DRIFTS/MS).

Experimental section

Preparation

Monometallic Ni-catalyst

The Ni, Mg, Al hydrotalcite-like precursor was prepared by coprecipitating an aqueous solution of nickel, magnesium and aluminum cations (solution A) with a highly basic carbonate solution (solution B) at room temperature. Solution A, containing $Ni(NO_3)_2{\cdot}6H_2O$, $Mg(NO_3)_2{\cdot}6H_2O$ and $Al(NO_3)_3{\cdot}9H_2O$ dissolved in distilled water was 1.5 M in (Al + Mg + Ni) with an Al/(Al + Mg) molar ratio equal to 0.25 and a Ni/Mg molar ratio of 1/1 [25]. Solution B was prepared by dissolving appropriate amounts of Na_2CO_3 and NaOH in distilled water in order to obtain a $[CO_3^{2-}]$ equal to 1.0 mol L^{-1} and a pH equal to 13 during the aging of the gel. In the synthesis procedure, solution A was slowly dropped (60 mL h^{-1}) under vigorous stirring to a B solution placed in a 150 mL PTFE reactor. The gel formed was aged under constant pH (13) for 18 h at 60 °C. The solid obtained was then filtered and washed with distilled water (90 °C) until pH 7 and then dried at 110 °C overnight.

The catalytically active form was obtained by reduction of the precursor under H_2 flow (30 mL min^{-1}), at 750 °C during 4 h and it was denoted as NiHT.

Pt–Ni bimetallic catalyst

The bimetallic catalyst was synthesized from NiHT reduced catalyst using techniques derived from Surface Organometallic Chemistry on Metals [26]. In this technique, the metallic precursor Pt acetylacetone (Pt $(acac)_2$) is decomposed through hydrogenation reaction (reaction (4)).

$$Pt(acac)_2 + 2Ni - H \rightarrow 2Ni - Pt + 2acacH \quad (4)$$

The hydrogen adsorbed on the surface of Ni reacts with Pt $(acac)_2$, producing acetylacetone (acacH) and Pt deposited on the metallic Ni. This allows the deposition of Pt selectively on the metallic Ni and not on the support. In this way, a bimetallic catalyst is achieved with a strong interaction between both metals and a high dispersion of Pt.

The method of preparation consisted of the reaction of 1 g of reduced NiHT catalyst with a solution of 0.06 wt% of Pt $(acac)_2$ in toluene at room temperature under flowing hydrogen during 6 h. Then, the liquid phase was separated and the solid was repeatedly washed with toluene and subsequently dried in a hydrogen flow at 90 °C and reduced in a hydrogen flow at 750 °C.

Catalytic tests and characterization

The steam reforming (SR) tests were carried out at atmospheric pressure in a continuous flow reactor. The reaction temperature was varied in the 450–600 °C range, keeping constant the feed composition (N_2/H_2O/EG equal to 7.4/31/1 in molar base) and the LHSV (1.72×10^5 mL h^{-1} g^{-1}).

The aqueous phase reforming (APR) was performed in a 100 mL high pressure batch reactor (BR-100 de Berghof Instruments). The reaction was studied at 250 °C and 44 bar and the feed was a solution of 10 wt% of EG. The analysis of gaseous products was performed with a Shimadzu GC-8A gas chromatograph equipped with a HayeSep DB 110–120 column and a GC/TCD detector. The liquid samples were analyzed by gas chromatography with CG/FID (Chrompack) and a mass spectrometry CG/MS detector (Shimadzu GCMS-QP5050A) with an HP-PONA capillary column (50 m). The accuracy of the measured values was within 5% and the experiments could be reproduced with a relative error of 10%.

The EG conversion is indicated as X_{EG} % and it was calculated based on the following equation:

$$X_{EG}\% = \frac{(\text{moles of EG in the feedstock} - \text{moles of EG in products})}{\text{moles of EG in the feedstock}} \times 100$$

The selectivity to H_2 is indicated as S_{H2} and it was calculated based on the following equation:

$$SH_2\ \% = \frac{\text{moles of } H_2 \text{ produced}}{\text{moles of EG reacted}} \times \frac{1}{5} \times 100$$

The selectivity of products indicated as S_{CO}, S_{CO2}, S_{CH4}, S_{CH3OH}, S_{C2H5OH} (%mol/mol) was calculated as produced moles of CO, CO_2, CH_4, CH_3OH and C_2H_5OH, respectively, divided by total moles of EG reacted *100

$$S_C\ \% = \frac{(\text{Mol of the product}) \times (\text{number of carbon atoms in the product})}{\text{mol of EG reacted} \times 2} \times 100$$

The simultaneous analyses of in situ Diffuse Reflectance Fourier Transform Infrared Spectroscopy (DRIFTS) and Mass Spectroscopy (MS) were carried out in a Nicolet spectrometer (Nexus 470) with a resolution of 4 cm^{-1} and an MCT-A detector. It was equipped with an accessory of diffuse reflectance and a chamber for heating up to high temperatures and ZnSe windows (Spectra-Tech). The effluent compounds from the DRIFTS chamber were continuously analyzed via a quadrupole mass spectrometer (Balzers QUADSTAR 422/QMS 200). The samples were treated in situ at 750 °C in flowing H_2 for 3 h (30 mL min^{-1}), followed by cooling to 350 °C in He flow

(30 mL min^{-1}). Ethylene glycol chemisorption was performed by exposing the catalyst to a flow of $C_2H_6O_2$/He mixture (30 mL min^{-1}) for 2 and 10 min.

After removing the reversibly adsorbed EG using He flow (30 mL min^{-1}) for 5 min, the catalyst was heated at different temperatures (400, 450, 500 and 550 °C) under a flow of He, and a spectrum was recorded (150 scans) in each step. The spectrum of the treated sample was used as background. The desorbing species were monitored by their characteristic mass fragmentation patterns (*m*/*z*): 2 (H_2); 18 (H_2O); 28 and 12 (CO); 31 (CH_3OH); 44 (CO_2); 33 ($C_2H_6O_2$). The fragment dominant of each desorbed product was qualitatively analyzed after being corrected for overlapping cracking fragments from other products.

The X-ray photoelectron spectroscopy (XPS) analyses were performed in a Multi-Technique UniSpecs equipment with a dual X-ray Mg/Al source and a PHOIBOS 150 hemispheric analyzer. The spectra were obtained with a pass energy of 30 eV and the Mg-Kα X-ray source was operated at 200 W and 12 kV. The working pressure in the analyzing chamber was less than 6×10^{-7} Pa. The binding energy (BE) of the C1s peak at 284.6 eV was taken as an internal standard.

The carbon deposits were studied using Laser Raman Spectroscopy (LRS) in a LabRAM HR UV 800 (Horiba/Jobin-Yvon) instrument, laser He–Ne ($\lambda = 632$ nm), CCD detector and an OLYMPUS microscope, model BX41. The measurements of the samples, diluted in KBr, were taken with a 100× magnification and the scattered light was collected through a confocal hole of 100 μm.

The carbon deposits were characterized by temperature-programmed oxidation (TPO), measuring the weight variation as a function of temperature in a thermogravimetric instrument (Shimadzu TGA 50). Post reaction samples of 0.010 g were used with air flow of 40 mL min^{-1} and heating of 10 °C min^{-1} from room temperature to 850 °C.

The chemical composition of the synthesized NiHT sample was determined by X-ray fluorescence (XRF) using a Rigaku spectrometer model Rix 3100, controlled by software Rix 3100, with an X-ray tube of Rh.

The Pt content in the PtNiHT sample was determined by Atomic Absorption (AA).

X-ray powder diffraction patterns were recorded in a Rigaku X-ray diffractometer with a graphite monochromator using Cu Kα radiation and varying 2θ values from 5 to 80°. The evaluation of the metallic phases was performed after the reduction of the samples ex-situ at 750 °C with pure H_2 (30 mL min^{-1}; 10 °C min^{-1}) for 60 min. The Rietveld method was used to quantify the phases formed [25].

Results and discussion

Crystalline phases and reducibility of Ni based catalysts

The general formula of the NiMgAl-hydrotalcite precursor was $Ni_{3.10}Mg_{3.12}Al_{1.78}(OH)_{16}(CO_3)_{0.89}$. X-ray diffraction results of the catalysts reduced ex-situ at 750 °C during 1 h in pure H_2, followed by the passivation process, are shown in Fig. 1. The analysis of the diffractogram of NiHT, indicates the presence of characteristic peaks of the periclase phase (MgO) at $2\theta = 36°$, 43°, 62°, 74° and 79° (JCPDS 75-1525) with a contribution of the spinel-phase ($MgAl_2O_4$) at $2\theta = 44°$, 74° and 78° (JCPDS 21-1152). With respect to Ni, the characteristic peaks of NiO at $2\theta = 37°$, 43° and 75°, (JCPDS 47-1049), and the segregation of the metallic Ni at 2θ = 44.6° and 51.8° (JCPDS 04-0850) are observed. The diffraction profile of the PtNiHT catalyst was similar to that of the NiHT catalyst (Fig. 1); and was not possible to determine any structural changes or the presence of a PtNi alloy. This is probably due to the very low content of Pt compared to the Ni content (Pt/Ni molar ratio = 0.0037).

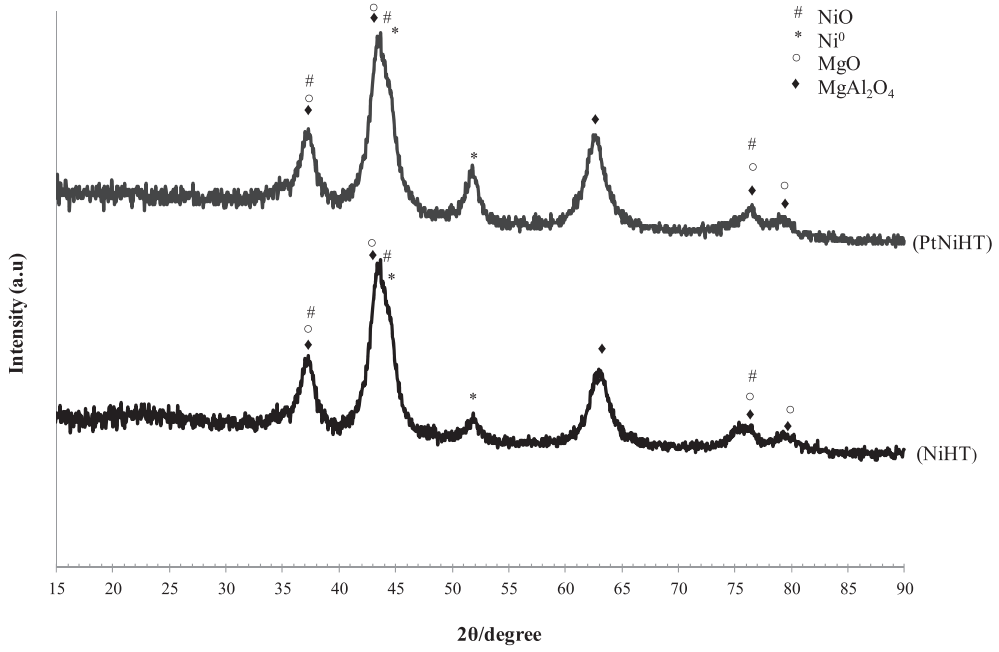

Fig. 1 – X-ray diffractograms of the NiHT and PtNiHT samples reduced ex-situ at 750 °C during 1 h in pure H_2 followed by passivation process.

The chemical composition obtained through the Rietveld refinement of XRD data was 40% Ni^0, 5.3% NiO, 54.8% $(MgAl)O_x$, and the Ni crystal size calculated from the diffraction peak at $2\theta = 51.8°$ was 6 nm. Using XRF, the composition was 51% NiO, 28% MgO and 20% Al_2O_3. The XRF results were consistent with those obtained from the application of the Rietveld method that enabled the relative quantification of the phases [25].

The PtNiHT catalyst was synthesized using a method derived from Surface Organometallic Chemistry on Metals using the NiHT solid, as described in the experimental section. The Pt content was 0.5 wt%, which led to a Pt/Ni molar ratio = 0.0037.

The TPR profiles exhibited a single reduction peak with maximum reduction at 730 °C and 720 °C for NiHT and PtNiHT respectively (Fig. 2). These profiles are very similar and hydrogen consumption would correspond to 60% reducibility for both samples. The peak at ~730 °C corresponds to reducing of nickel species Ni^{2+} to Ni° and can be associated either to the reduction of $NiAl_2O_4$ spinel phase [27] or to the reduction of nickel atoms located in Mg–Ni–O solid solution [28,29]. Such temperature is much higher than that for pure NiO, which is reduced at 300–450 °C, demonstrating a strong interaction of the nickel species with the mixed oxide matrix [30].

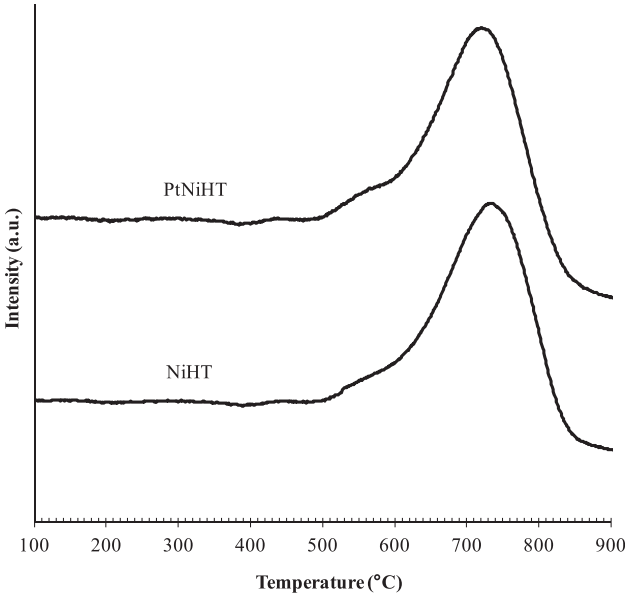

Fig. 2 – Temperature programmed reduction (TPR) profiles for NiHT and PtNiHT catalysts.

SR and APR of ethylene glycol

As indicated in the experimental section, NiHT and PtNiHT catalysts were tested in both the steam reforming (SR) and the aqueous phase reforming (APR) reactions of ethylene glycol. The catalysts were pre-reduced at 750 °C during 3 h under pure hydrogen flow.

Table 1 shows the results of the ethylene glycol conversion (X_{EG}) and the product selectivity measured at different reaction temperatures. The reaction products identified were H_2, CO, CO_2, CH_4, CH_3OH and C_2H_5OH. Most of the products were in the gas phase, and the major component was H_2. As expected, the gas composition depended on the reaction conditions (SR or APR). Carbon balance for all runs are listed in Table 1, were close to within 6%. The steam reforming of EG was carried out at 450, 525 and 600 °C, which is a favorable condition to C–C cleavage reactions. The conversion levels at 525 and 600 °C are very high for both catalysts, however the selectivity to CO_2 is higher for the PtNiHT catalyst. At 450 °C, lower conversions are achieved and it can be seen that the PtNiHT catalyst was more active than NiHT, with higher H_2 and CO_2 selectivity. This could indicate a higher contribution of the WGS reaction (reaction (2)) due to the presence of Pt.

The aqueous phase reforming reaction of EG was carried out at 44 bar and 250 °C, which are favorable conditions to WGS reaction (reaction (2)) and to C–O cleavage reaction (as the methanation, reaction (3)). The results for both catalysts showed that the main products in the gaseous phase were H_2 and CO_2, with a very low content of CO and higher content of CH_4 than SR. The presence of Pt confers a higher activity to the catalyst, but decreases the selectivity to H_2. This could be explained by a higher selectivity to liquid products (mainly ethanol), which could indicate a higher contribution of C–O bond cleavage reactions.

Our results are in agreement with those reported by Li et al. [11], which indicate that at temperatures higher than 500 °C it is possible to obtain EG conversions higher than 90% employing Ni catalysts. However, these authors reported that when the temperature decreases, methanol, ethylene, acetaldehyde, ethanol and acetone appear depending on the type of support. The acid sites of the support would favor dehydration reactions to produce acetaldehyde and ethylene, and these compounds are precursors of carbon deposits. The

Table 1 – Catalytic tests.

Catalyst	Temp (°C)	X_{EG}	S_{H2}	S_{CO}	S_{CH4}	S_{CO2}	S_{CH3OH}	S_{C2H5OH}	C balance, out/in (%)
NiHT	450[a]	71	69.5	27.8	18.3	44.7	9.2	0	99
PtNiHT	450[a]	89	84.6	22.8	5.6	70.9	0.7	0	97
NiHT	525[a]	86	86.4	14.2	5.4	80.4	0	0	95
PtNiHT	525[a]	92	89.8	1.0	6.2	92.8	0	0	95
NiHT	600[a]	89	96.5	8.3	2.6	89.1	0	0	94
PtNiHT	600[a]	94	96.1	6.0	0.3	93.7	0	0	94
NiHT	250[b]	49	91.8	1.1	23.1	69.7	5.4	0.7	99
PtNiHT	250[b]	58	56.1	0.6	22.6	66.5	6.1	4.2	99

[a] Results after 2 h of reaction, $\tau = 0.36$ min, total flow fed 288 cm^3/min ($N_2/H_2O/EG = 7.4/31/1$).
[b] Test in liquid phase at 44 bar N_2.

lowest content of methanol and ethanol observed in the tests could be explained by the fact that the hydrotalcite like-compounds do not have acidic properties.

Some authors have also indicated the presence of acetic acid as the main intermediate compound of coke [19]. However, we did not detect acetic acid in the liquid products.

To better understand the catalyst performance, a combination of in situ DRIFTS and Mass Spectrometry analyses of ethylene glycol adsorption was carried out. Special attention was paid to intermediate species formation and surface activity since in situ infrared data can provide evidence for the reaction mechanism that involves adsorbed surface species and conversion of the reactant molecule.

The DRIFT spectra obtained after EG adsorption on the NiHT catalyst show (Fig. 3) bands at 3673 cm^{-1} due to the OH stretching vibration, and other bands at 1437 and 1532 cm^{-1} assigned to carboxylate species (1560–1630 cm^{-1} – ν_a COO^-; 1350–1420 cm^{-1} – ν_s COO^-). The shoulders at 1382 and 1540 cm^{-1} (*) could be attributed to formate species. The mass spectra (Fig. 4) show the formation of H_2, CO_2, methanol and H_2O during the EG adsorption step and after the reversible species are removed with He flow.

After heating the sample, the DRIFT spectra show that the decomposition of the adsorbed species occurs above 500 °C with an increase in the formation of CO_2 in the gas phase (Fig. 5). The bands due to formate adsorbed species remain at 550 °C, suggesting that these intermediate species are strongly adsorbed. The stability of the formate species could be responsible for the low catalytic activity of the NiHT sample.

On the other hand, the spectra of EG adsorbed on the PtNiHT sample (Fig. 6) show a less intense band corresponding to formate species (~1550 and 1390 cm^{-1}) while the bands regarding to carboxylates are not observed. Mass spectra (Fig. 7) indicate that methanol was not produced, which is in agreement with the results of the SR reaction. This suggests that the PtNiHT catalyst is more active to decompose the carboxylate and formate species than the NiHT catalyst, resulting in an increased activity for the steam reforming reaction. Jacobs and Davis indicated that the decomposition of formate is the limiting step in the WGS reaction [31]. According to the DRIFTS results for the PtNiHT catalyst, the formate bands show low intensity, and this could explain the higher activity of this catalyst to produce CO_2 by the WGS reaction.

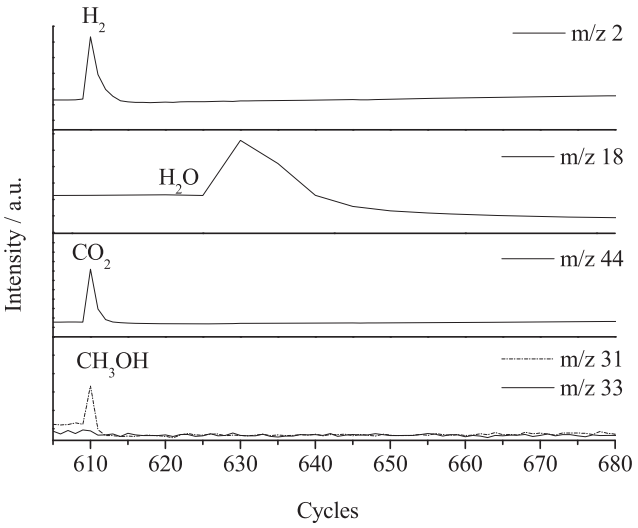

Fig. 4 – MS analyses during EG adsorption for NiHT at 350 °C; cycles from EG adsorption (2 min–10 min); characteristic mass fragmentation patterns (*m/z*): 2 (H_2); 18 (H_2O); 31 (CH_3OH); 44 (CO_2); 33 ($C_2H_6O_2$).

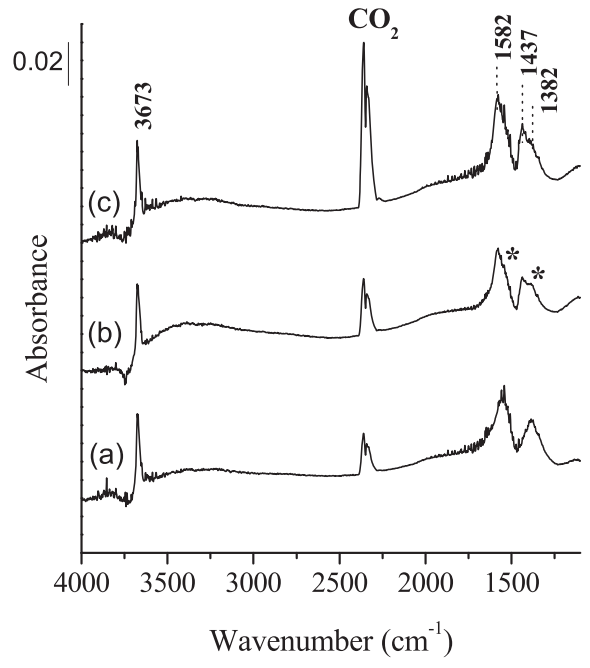

Fig. 3 – DRIFT spectra of EG adsorption on NiHT at 350 °C: (a) EG adsorption (2 min); (b) 10 min; (c) He flow (5 min).

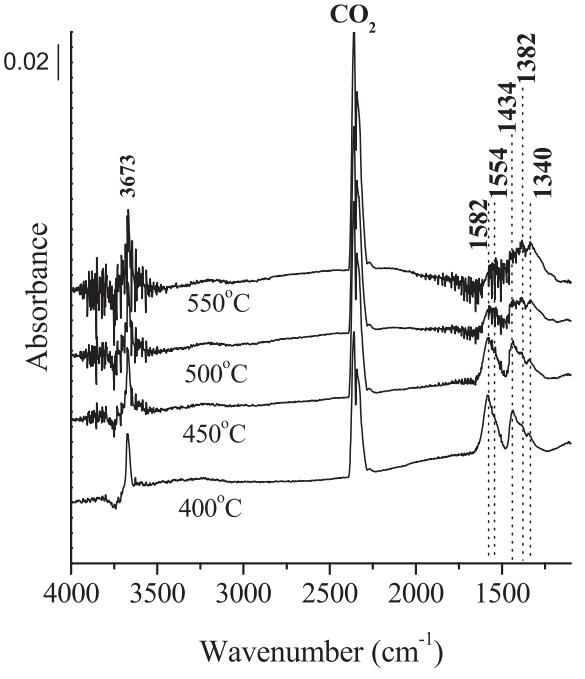

Fig. 5 – DRIFT spectra of EG desorption from NiHT in He flow (400–550 °C).

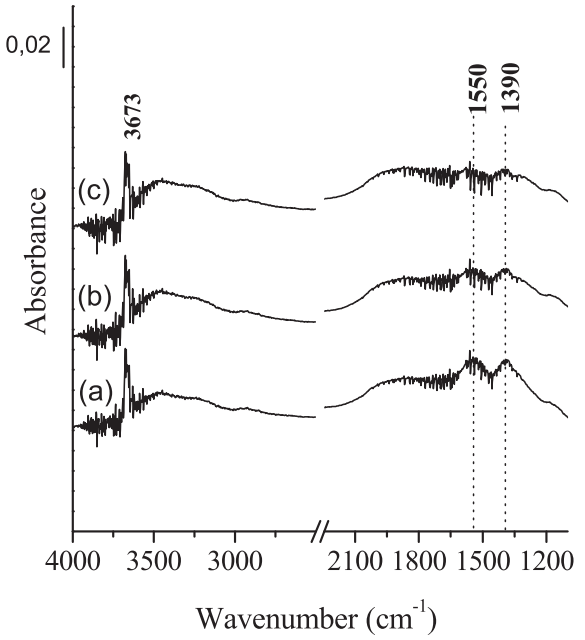

Fig. 6 – DRIFT spectra of EG adsorption for PtNiHT at 350 °C: (a) EG adsorption (2 min); (b) 10 min; (c) He flow (5 min).

Characterization of catalysts used in the SR of ethylene glycol

The fresh reduced samples and those used during 6 h in the SR reaction were characterized through XPS. The surface ratio of the different species are shown in Table 2. In all samples, the peak of Mg 2p appears at 49.5 eV. On the other hand, Pt could not be detected probably due to the overlapping between the corresponding signals to Al 2p, Ni 3p and Pt 4f.

The region of Ni $2p_{3/2}$ presents three peaks (Fig. 8): a wide peak corresponding to the shake-up satellite, and two peaks, one at 855.5 eV assigned to Ni(II), strongly interacting with the support, and another at 852 eV that corresponds to Ni in its reduced state [32,33]. Noteworthy, it is possible that an alloy was formed in the PtNiHT catalyst obtained by the SOMC/M preparation technique. However, a noticeable shift in the BE of Ni was not observed probably due to the low content of Pt (Pt/Ni = 0.0037). It can also be observed that after reaction the catalysts showed a lower proportion of Ni^0 due to the partial covering by carbon deposits.

Table 2 – XPS characterization of fresh and used aliquots of mono and bimetallic formulations.

Catalyst[a]	Ni/Mg	[b]Ni(0)/Ni(II) + Ni(0)	Al/Mg
NiHT	0.19	1	0.80
PtNiHT	0.15	1	0.81
PtNiHT450	0.27	0.1	0.67
NiHT450	0.32	0.1	0.72
PtNiHT600	0.39	0.1	0.87
NiHT600	0.12	0.25	0.80

[a] Numbers refer to reaction temperatures.
[b] Ni(II) (BE = 855.3 eV) and Ni(0) (BE = 851.8 eV), Mg 2p (BE = 49.5 eV).

Table 2 also reports the Ni/Mg and Al/Mg surface atomic ratios. After all treatments, the Al/Mg ratio was higher than the bulk value (Al/Mg = 0.33). This behavior was previously assigned to the higher mobility towards the surface of aluminum oxide during the calcination and reduction of Ni–Mg–Al hydrotalcites like compounds [34].

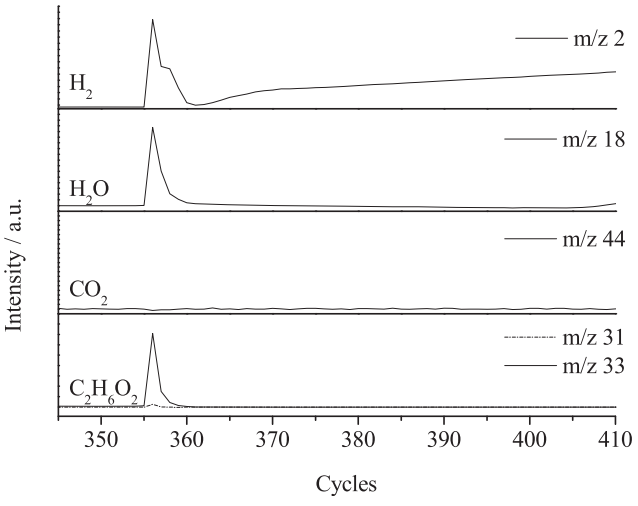

Fig. 7 – MS analyses during EG adsorption for PtNiHT at 350 °C; cycles from EG adsorption (2 min–10 min); characteristic mass fragmentation patterns (*m/z*): 2 (H_2); 18 (H_2O); 31 (CH_3OH); 44 (CO_2); 33 ($C_2H_6O_2$).

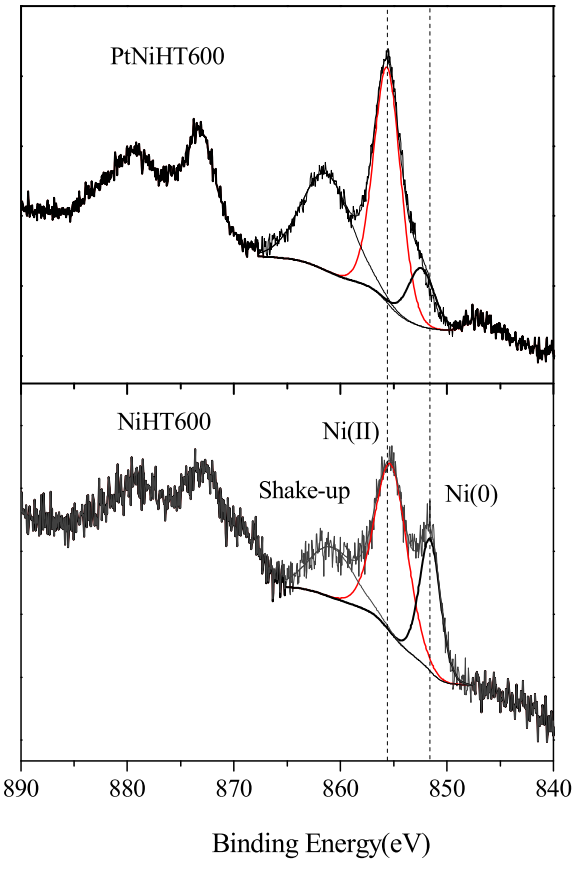

Fig. 8 – XPS Ni 2p spectra for PtNiHT and NiHT catalysts after been used in the SR of EG at 600 °C.

The carbon deposits were investigated by laser Raman spectroscopy and thermogravimetric analyses (Fig. 9). The carbon species showed Raman bands in the range of 1000–1700 cm^{-1}. According to the literature, the band at 1560 cm^{-1} (G band) is related to the stretching vibration mode E2g in C=C (C sp2) and the band at 1360 cm^{-1} (D band) refers to the A2g mode due to the breathing mode of a six-fold ring [35,36]. The Raman spectra samples after the SR reaction at 450 °C did not show significant differences in the carbon species formed, with characteristic disordered graphitic carbon bands at 1360 cm^{-1} (C sp3) and characteristic ordered graphitic carbon bands at 1600 cm^{-1} (C sp2) for both samples. The intensity ratio I_D/I_G is maintained between 0.99 and 1.05 for NiHT and PtNiHT respectively.

The content of carbon in the used samples was determined through thermogravimetric analyses, TPO/TGA. The registered weight loss at temperatures higher than 500 °C was assigned to the combustion of the carbon deposits. The maximum burning temperatures were very similar for all samples (Table 3), in agreement with the Raman spectra indicating the similarity in the nature of carbon. When the SR reaction was carried out at 450 °C, the carbon content was very similar for both catalysts, around 2 wt%C. The presence of 0.5% of Pt in the bimetallic catalyst did not inhibit the formation of carbon.

At high reaction temperatures (525 and 600 °C), tests of EG thermal decomposition (without the catalyst) were carried out. These experiments showed the formation of acetaldehyde, products with higher molecular weight than EG and carbon deposits. As a consequence, the carbon content determined by TPO/TGA in samples used at high reaction temperatures (Table 3) partly comes from the thermal decomposition of the ethylene glycol. This does not allow a correct assessment of the amount of carbon formed. Then, to study the stability of the PtNiHT catalyst, it would be convenient to conduct the SR reaction at 450 °C, although only a lower selectivity to hydrogen (~85%) is achieved under these conditions.

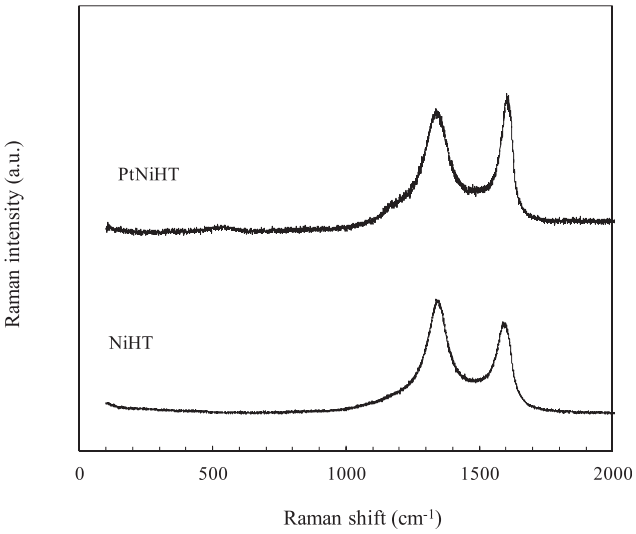

Fig. 9 – Laser Raman spectra of PtNIHT450 and NiHT450.

Table 3 – Carbon content in the used samples calculated from TPO/TGA data.

Catalyst	%C	Maximum burning temperature (°C)
NIHT250	<0.1	
NiHT450	1.5	550
NiHT525	2.8	532
NIHT600	3.1	555
PtNiHT250	<0.1	
PtNiHT450	1.7	550
PtNiHT525	7.0	546
PtNiHT600	6.8	554

TPO/TGA conditions: air flow of 40 mL min^{-1} and heating of 10 °C min^{-1} from room temperature to 850 °C.

Conclusions

The PtNiHT catalyst was synthesized using a well-controlled technique (SOMC/M). This methodology allows obtaining well-defined active phases, with low Pt/Ni ratio (~0.004).

The PtNiHT catalyst was promising for the production of hydrogen from the SR reaction at 450 °C, because it was more active and selective to hydrogen than NiHT and promoted the WGS reaction. Under the APR conditions of ethylene glycol (high pressure and low temperature), the presence of Pt gives higher catalyst activity and causes a decrease in the selectivity to hydrogen due to higher selectivity to methane and to liquid products by C–O bond cleavage reactions.

Through the DRIFT studies during the ethylene glycol adsorption/desorption, a low stability of the formate and carboxylate species was observed in the PtNiHT catalyst. Thus, as the formate decomposition is the limiting step in the WGS reaction, this would explain the higher activity of PtNiHT to produce CO_2 through WGS.

At higher temperatures, 525 and 600 °C, thermal decomposition and condensation reactions were favored, which would originate carbon deposits.

Acknowledgments

We are grateful for the funding received from the CONICET/CNPq International Cooperation Joint Project (res 457/12).

REFERENCES

[1] Lu YJ, Guo LJ, Ji CM, Zhang XM, Hao XH, Yan QH. Hydrogen production by biomass gasification in supercritical water: a parametric study. Int J Hydrogen Energy 2006;31:822–31.
[2] Zhang B, Tang X, Li Y, Xu Y, Shen W. Hydrogen production from steam reforming of ethanol and glycerol over ceria-supported metal catalysts. Int J Hydrogen Energy 2007;32:2367–73.
[3] Shabaker JW, Davda RR, Huber GW, Cortright RD, Dumesic JA. Aqueous-phase reforming of methanol and ethylene glycol over alumina-supported platinum catalysts. J Catal 2003;215:344–52.

[4] Davda RR, Shabaker JW, Huber GW, Cortright RD, Dumesic JA. Aqueous-phase reforming of ethylene glycol on silica-supported metal catalysts. Appl Catal B Environ 2003;43:13–26.
[5] Basagiannis AC, Verykios XE. Catalytic steam reforming of acetic acid for hydrogen production. Int J Hydrogen Energy 2007;32:3343–55.
[6] Klouz V, Fierro V, Denton P, Katz H, Lisse JP, Bouvot-Mauduit S, et al. Ethanol reforming for hydrogen production in a hybrid electric vehicle: process optimization. J Power Source 2002;105:26–34.
[7] Ni M, Leung DYC, Leung MHK. A review on reforming bio-ethanol for hydrogen production. Int J Hydrogen Energy 2007;32:3238–47.
[8] Shabaker JW, Huber GW, Davda RR, Cortright RD, Dumesic JA. Aqueous-phase reforming of ethylene glycol over supported platinum catalysts. Catal Lett 2003;88:1–8.
[9] Kandoi S, Greeley J, Simonetti D, Shabaker J, Dumesic JA, Mavrikakis M. Reaction kinetics of ethylene glycol reforming over platinum in the vapor versus aqueous phases. J Phys Chem C 2011;115:961–71.
[10] Christiansen MA, Vlachos DG. Microkinetic modeling of Pt-catalyzed ethylene glycol steam reforming. Appl Catal A General 2012;431:18–24.
[11] Li S, Zhang C, Zhang P, Wu G, Ma X, Gong J. On the origin of reactivity of steam reforming of ethylene glycol on supported Ni catalysts. Phys Chem Chem Phys 2012;14:4066–9.
[12] Tupy SA, Chen JG, Vlachos DG. Comparison of ethylene glycol steam reforming over Pt and NiPt catalysts on various supports. Top Catal 2013;56:1644–50.
[13] Cortright RD, Davda RR, Dumesic JA. Hydrogen from catalytic reforming of biomass-derived hydrocarbons in liquid water. Nature 2002;418:964–7.
[14] de Vlieger DJM, Chakinala AG, Lefferts L, Kersten SRA, Seshan K, Brilman DFW. Hydrogen from ethylene glycol by supercritical water reforming using noble and base metal catalysts. Appl Catal B 2012;12:536–44.
[15] Huber GW, Shabaker JW, Dumesic JA. Raney Ni-Sn catalyst for H_2 production from biomass-derived hydrocarbons. Science 2003;300:2075–7.
[16] Shabaker JW, Huber GW, Dumesic JA. Aqueous-phase reforming of oxygenated hydrocarbons over Sn-modified Ni catalysts. J Catal 2004;222:180–91.
[17] Shabaker JW, Dumesic JA. Kinetics of aqueous-phase reforming of oxygenated hydrocarbons: Pt/Al_2O_3 and Sn-modified Ni catalysts. Ind Eng Chem Res 2004;43:3105–12.
[18] Shabaker JW, Simonetti DA, Cortright RD, Dumesic JA. Sn-modified Ni catalysts for aqueous-phase reforming: characterization and deactivation studies. J Catal 2005;231:67–76.
[19] de Vlieger DJM, Mojet BL, Lefferts L, Seshan K. Aqueous phase reforming of ethylene glycol – role of intermediates in catalyst performance. J Catal 2012;292:239–45.
[20] Chu X, Liu J, Sun B, Dai R, Pei Y, Qiao M, et al. Aqueous-phase reforming of ethylene glycol on Co/ZnO catalysts prepared by the coprecipitation method. J Mol Catal A Chem 2011;335:129–35.
[21] Nawfal M, Gennequin C, Labaki M, Nsouli B, Aboukais A, Abi-Aad E. Hydrogen production by methane steam reforming over Ru supported on Ni-Mg-Al mixed oxides prepared via hydrotalcite route. Int J Hydrogen Energy 2015;40:1269–77.
[22] Jun Z, Ning Z, Wei W, Yuhan S. Partial oxidation of methane over Ni/Mg/Al/La mixed oxides. Prepared from layered double hydrotalcites. Int J Hydrogen Energy 2010;35:11776–86.
[23] Li D, Koike M, Chen J, Nakagawa Y, Tomishige K. Preparation of Ni-Cu/Mg/Al catalysts from hydrotalcite-like compounds for hydrogen production by steam reforming of biomass tar. Int J Hydrogen Energy 2014;39:10959–70.
[24] Mei D, Lebarbier Dagle V, Xing R, Albrecht KO, Dagle RA. Steam reforming of ethylene glycol over $MgAl_2O_4$ supported Rh, Ni, and Co catalysts. ACS Catal 2016;6:315–25.
[25] Cesar DV, Baldanza MAS, Henriques CA, Pompeo F, Santori G, Munera J, et al. Hydrogen and/or syngas from steam reforming of glycerol. Study of platinum catalysts. Int J Hydrogen Energy 2013;38:5616–26.
[26] Womes M, Cholley T, Le Peltier F, Morin S, Didillon B, Szydlowski-Schildknecht N. Study of the reaction mechanisms between $Pt(acac)_2$ and alumina surface sites: application to a new refilling technique for the controlled variation of the particle size of Pt/Al_2O_3 catalysts. Appl Catal A Gen 2005;83:9–22.
[27] Rodrigues AC, Henriques CA, Monteiro JL. Influence of Ni content on physico-chemical characteristics of Ni, Mg, Al-hydrotalcite like compounds. Mater Res 2003;4:563–8.
[28] Takehira K, Shishido T, Wang P, Kosaka T, Takaki K. Autothermal reforming of CH_4 over supported Ni catalysts prepared from Mg–Al hydrotalcite-like anionic clay. J Catal 2004;221:43–54.
[29] Schulze K, Makowski W, Chyży R, Dziembaj R, Geismar G. Nickel doped hydrotalcites as catalyst precursors for the partial oxidation of light paraffins. Appl Clay Sci 2001;18:59–69.
[30] Dussault L, Dupin JC, Guimon C, Monthioux M, Latorre N, Ubieto T, et al. Development of Ni–Cu–Mg–Al catalysts for the synthesis of carbon nanofibers by catalytic decomposition of methane. J Catal 2007;251:223–32.
[31] Jacobs G, Davis BH. In situ DRIFTS investigation of the steam reforming of methanol over Pt/ceria. Appl Catal A 2005;285:43–9.
[32] Romero A, Jobbagy M, Laborde M, Baronetti G, Amadeo N. Ni(II)–Mg(II)–Al(III) catalysts for hydrogen production from ethanol steam reforming: influence of the activation treatments. Catal Today 2010;149:407–12.
[33] Fan L, Liu PF, Yan X, Gu L, Yang ZZ, Yang HG, et al. Atomically isolated nickel species anchored on graphitized carbon for efficient hydrogen evolution electrocatalysis. Nat Commun 2016;7:10667. http://dx.doi.org/10.1038/ncomms10667.
[34] Jirátová P, Cuba F, Kovanda L, Pitchon H. Preparation and characterisation of activated Ni (Mn)/Mg/Al hydrotalcites for combustion catalysis. Catal Today 2002;76:43–53.
[35] Narksitipan S, Thongtem T, Thongtem S. Characterization of sp3 carbon produced by plasma deposition on gamma-TiAl alloys. Appl Surf Sci 2008;254:7759–64.
[36] Arepalli S, Nikolaev P, Gorelik O, Hadjiev V, Holmes W, Files B, et al. Protocol for the characterization of single-wall carbon nanotube material quality. Carbon 2004;42:1783–91.